Y. Watanabe, T. Kazama: 2011 ERK2 Contributes to the Control of Social Behaviors in Mice. The Journal of Neuroscience, 31, 11953-11967.

5. N. Takashima, Y. S. Odaka, K. Sakoori, T. Akagi, T. Hashikawa, N. Morimura, K. Yamada, J. Aruga: 2011 Impaired cognitive function and altered hippocampal synapse morphology in mice lacking *Lrrtml*, a gene associated with schizophrenia. PLoS ONE, 6, e22716.

6. T. Sano, Y-J. Kim, E. Oshima, C. Shimizu, Kiyonari. H, T. Abe, H. Higashi, K. Yamada, Y. Hirabayashi: 2011 Comparative characterization of GPRC5B and GPRC5C LacZ knockin mice; Behavioral abnormalities in GPRC5B-deficient mice. BBRC, 412, 460-465.

2. 学会発表 (発表誌名、巻号、ページ、発行年も記入)

国際学会:

1. N. H. Tomioka, K. Yamada, M. Ota, Y. S. Odaka, J. Aruga: 2011 Characterization of Elfn family in the central nervous system. Neuroscience 2011, the Society for Neuroscience 41th Annual Meeting, (Washington, DC, November 12-16, 2011)

2. I. Ogiwara, S. Tto, K. Yamada, K. Yamakawa: 2011 Nav1.1-haploinsufficient mice, a model for Dravet syndrome, exhibit l earning impairment and autistic -like behaviors. Neuroscience 2011, the Society for Neuroscience 41th Annual Meeting, (Washington, DC, November 12-16, 2011)

3. J. Aruga, N. Takashima, Y. S. Odaka, K. Sakoori, T. Akagi, T. hashikawa, N. Morimura, K. Yamada: 2011 Neuroscience 2011, the Society for Neuroscience 41 th Annual Meeting, (Washington, DC, November 12-16, 2011)

国内学会:

1. 本間千尋、山田一之:2011 連続空間内でのマウス(*Mus musclus*) の行動と薬物作用評価の検討 Animal 2011 (第71回日本動物心理学会大会、第30回日本動物行動学会、2011年度応用動物行動学会/日本家畜学会 合同大会) ポスター発表 (9月8-11日 慶応大学)

2. N. Morimura, H. Yasuda, K. Yamada, N. H. Tomioka, K-I. Katayama, K. Yamaguchi, M. Ota, A. Kamiya, J. Aruga: 2011 Lrfn2/SALM1 regulates excitatory synapse function in the hippocampus and its deficient mice display mental disorder -like behav ioral abnormalities. 第34回日本神経科学大会 シンポジウム (9月14-17日 パシフィコ横浜)

3. M. Hatayama, A. Ishiguro, Y. Iwayama, N. Takashima, K. Sakoori, T. Toyota, Y. Nozaki, Y. S. Odaka, K. Yamada, T. Yoshikawa, J. Aruga: 2011 Zic2 hypomorphic mutant mice as a schizophrenia model and ZIC2 mutations identified in schizophrenia patients. 第34回日本神経科学大会 口頭発表 (9月14-17日 パシフィコ横浜)

4. Y. Matsumoto, K-Ichi Katayama, T. Okamoto, K. Yamada, S. Nagao, M. Kudoh: 2011 Auditory and Vestibular Impairment of *Slitrk6*-Deficient Mice. 第34回日本神経科学大会 ポスター発表 (9月14-17日 パシフィコ横浜)

5. N. Takashima, Y. Odaka, K. Sakoori, T. Akagi, T. Hashikawa, N. Morimura, K. Yamada, J. Aruga: 2011 Executive dysfunction in novel environment and altered hippocampal synapse morphology in mice lacking Lrrtml. 第34回日本神経科学大会 ポスター発表 (9月14-17日 パシフィコ横浜)

6. N. H. Tomioka, K. Yamada, M. Ota, Y. S. Okada, J. Aruga: 2011 Characterization of Elfn

family in the central nervous system. 第34回日本分子生物学会年会 (12月13-16日 パシフィコ横浜)

7. 畑山実、石黒亮、岩山佳美、高嶋紀子、佐郡和人、豊田倫子、野崎弥生、小高由梨、 山田一之、吉川武男、有賀純 第34回日本分子生物学会年会 (12月13-16日 パシフィコ横浜)

H. 知的財産所有権の出願・登録状況 (予定も含む)

1. 特許取得

なし

2. 実用新案登録

なし

3. その他

なし

平成23 年度厚生労働科学研究費補助金（化学物質リスク研究事業）
神経系発生−発達期の化学物質暴露による遅発中枢影響解析に基づく
統合的な情動認知行動毒性評価系確立に資する研究（H23−化学−一般−004）

発生−発達期ビスフェノールA 暴露の行動発達に対する影響解析

独立行政法人理化学研究所
脳科学総合研究センター
山田一之

1．目的

・プラスチック原料の一種であるビスフェノールA（以下BPA）は、製品から溶出して生体内に取り込まれると、エストロジェン受容体に結合してホルモン類似作用を呈すると考えられている。

→内分泌かく乱物質の代表的化合物の一つ

・基礎研究から大規模な疫学調査に至る多くの研究が行われて来たが、BPAの神経系への影響については未だに不明な点が多い。

→生殖や身体発達における影響が注目され、中枢への影響について余り調べられていない

→低容量効果説（薬理学的作用量を大幅に下回る低用量でも生体に影響を及ぼすという説）については、議論が分かれている

☆近年急速に注目を集めつつある小児毒性学的視点を踏まえて、胎生期から離乳期における母体へのBPA暴露が、仔の発達と認知・情動機能に及ぼす影響について、マウスをモデル実験系として検討することを目的とした。

2. 方法

マウス購入 :C57BL/6J（日本クレア）、6週齢（♂、♀合計各40匹）

↓

馴致 :1週間（飼育条件：明暗周期12時間（午前8時点灯）、温度22±1℃、湿度50-60%；以下同じ）

↓

交配 :10日間：11日目の午後に♂マウスと分離

↓

出産 :妊娠確認後、毎朝妊娠個体の状態を調べ、出産が確認された日を生後0日 (PD0)とした

↓

乳幼児期実験 :PD 5から体重測定および下記の観察・評価を行った

PD 5: 正向反射、把握反射
PD 8: クリック驚愕反射
PD13:オープンフィールド試験、開眼確認（PD12-）
PD18:新奇物体認識試験

正向反射
(righting reflex)
From Ronca AE & Alberts JR
(2000)

↓

離乳 :PD28

↓

成体期実験* :生後8週齢から行動テストバッテリによる行動解析を開始

内容：ホームケージ自発活動性測定、オープンフィールド試験、明暗往来試験、高架式十字迷路試験、聴覚性驚愕反応およびそのプレパルス抑制試験、恐怖条件付け試験、MRI測定

*乳幼児器の経験バイアスを避けるため、成体期実験は乳幼児期実験と異なる個体を用いた。

3.結果

category/task		vehicle	BPA
infant (-PD18)			
body weight			< (statistically significant)
righting reflex (PD5)		○	○
click startle response (PD8)		△	△
eye opening (PD13)			< (statistically significant)
open field (PD13)			n.s.
novelty/object test (PD18)			n.s.

category/task		vehicle	BPA
adult (8 weeks-)			
body weight			<
HC activity			<
open field			n.s.
L-D box			n.s.
elevated plus maze			n.s.
auditory startle &PPI			< (startle only)
fear conditioning	conditioning		n.s.
	context test		< (partially)
	cued test		< (partially)

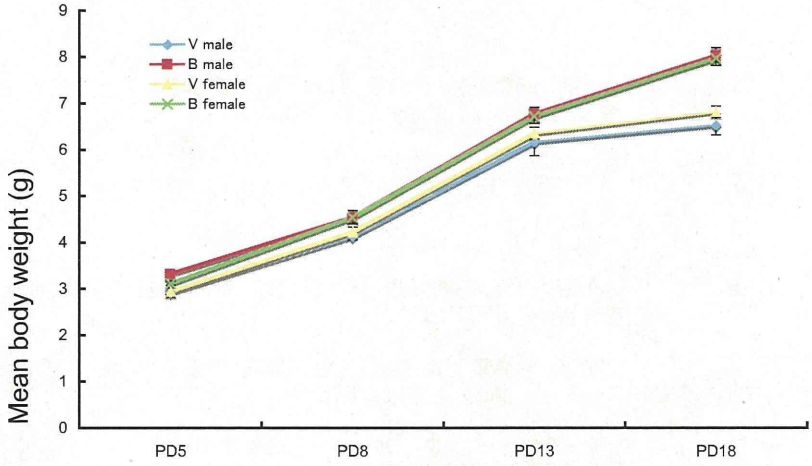

Fig. 1 授乳期における体重変化

データは平均と±標準誤差を示す。(PD5:F(1,49)=15.7, p<0.0001; PD8:F(1,49)=8.67, p<0.005, PD13:F(1,49)=7.91, p<0.01; PD18:F(1,49)=66.5, p<0.0001)

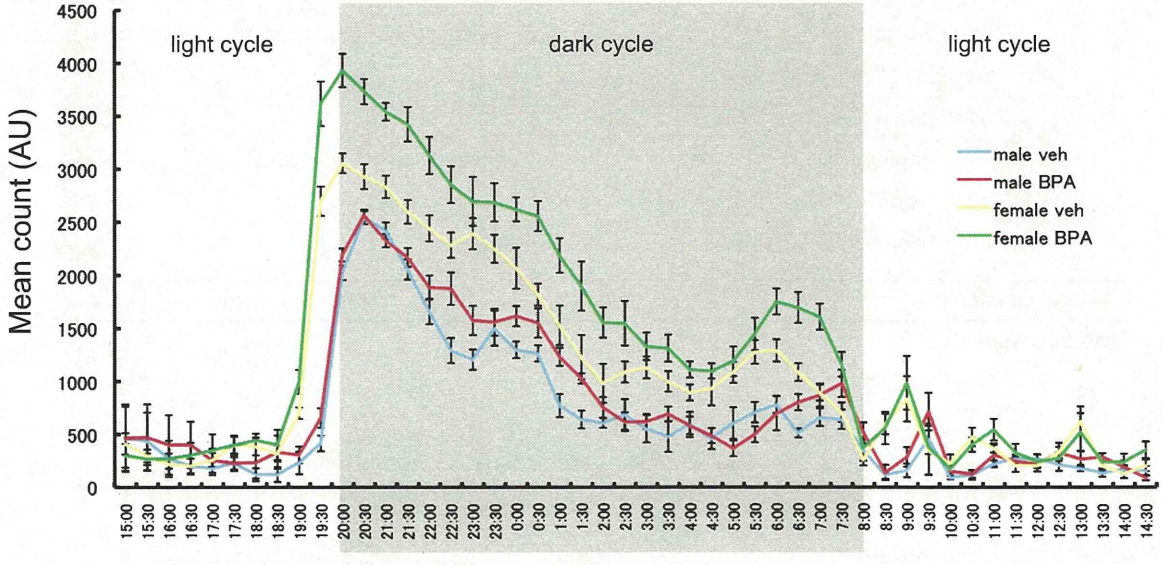

Fig. 2 ホームケージ自発活動性測定の結果

データは平均と±標準誤差を示す。3元配置の分散分析(性別 × 処置 × 日)の結果、性別 (F(1,6)=591.7, p<0.001)、処置 (F(1,6)=106.3, p<0.001) の主効果、および性 × 処置の交互作用 (F(1,6)=20.1, p<0.01)が有意であった。

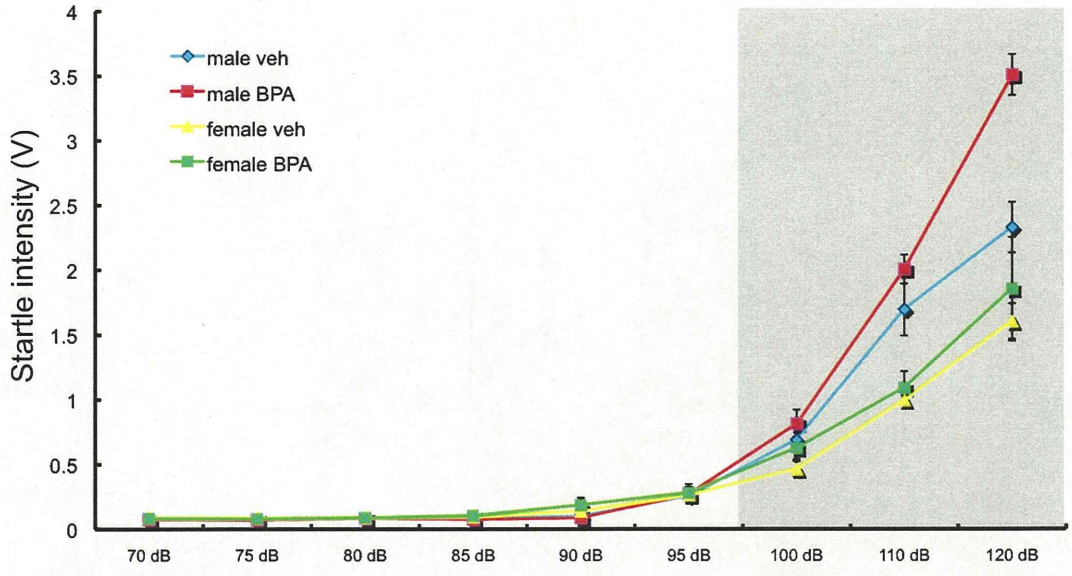

Fig. 3 聴覚性驚愕反応測定の結果

データは平均と±標準誤差を示す。3元配置の分散分析（100 dB から 120 dB: 性別 × 処置 × 日）の結果、性別 ($F(1,87)=55.1$, $p<0.001$)、処置 ($F(1,87)=12.7$, $p<0.001$)、および音圧 ($F(2,87)=88.7$, $p<0.001$)の主効果が有意であった。.

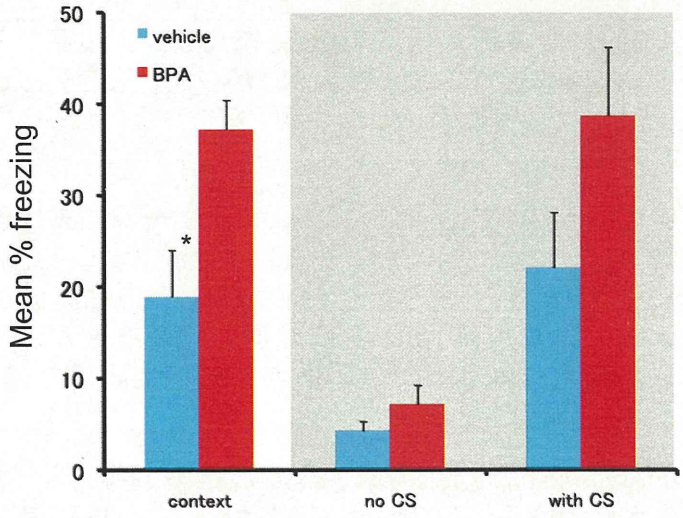

Fig. 4 恐怖条件付けの結果

データは平均と±標準誤差を示す。2元配置の分散分析 (処置 x 時間枠) の結果、処置 (文脈（場所）テスト：$F(1,78)=21.6$, $p<0.01$；手掛かり（音）テスト：$F(1,52)=6.7$, $p<0.05$) と時間枠 (文脈（場所）テスト：$F(5,78)=5.92$, $p<0.01$； 手掛かり（音）テスト$F(3,52)=5.40$, $p<0.01$)の有意な主効果が認められた。*：vehicle群とBPA群の間の差 (Mann Whitney's U-test: $p<0.05$)。

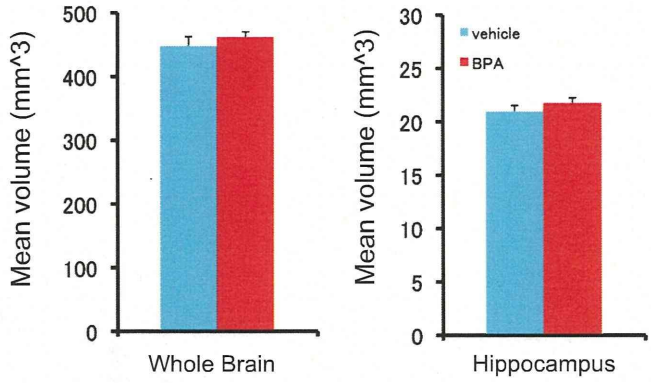

Fig. 5 MRI測定の結果

データは平均±標準誤差を示す。全脳容積および海馬容積について、vehicle群とBPA群に有意な差は認められなかった。

4. 考察

1）乳幼児期については、行動変化は見いだせなかったが、体重の増加傾向や開眼時期の早期化といった発達加速的な傾向が見られた。本研究はマウスを用いたモデル研究であり、またサンプル集団もそれほど大きくないので、結論を出すことはできないが、更なるモデル研究に加えて、今一度これまでに蓄積されたヒトに関するデータについて再検討することも重要と考えられる。

2）成体期においてはBPA添加群において、飼育ケージにおける自発活動性・聴覚性驚愕反応・恐怖条件付け後の恐怖反応（すくみ反応）に有意な亢進が見られた。驚愕刺激に対する過剰な反応や恐怖反応の亢進は、心的外傷後ストレス障害(PTSD)等に関連する可能性が報告されているので、これらの変化に対するBPAの関与について詳細な追加検討が必要である。

3）ヒトにおけるPTSDの臨床研究では、画像診断によって脳容積の減少等の変化が報告されている。そこで、本研究においても核磁気共鳴法による脳画像分析を試みたが、形態・容積ともに変化を見出すことはできなかった。

5. 結論

胎生期および授乳期に母体がビスフェノールA暴露を受けた場合、その仔の身体的発達および成長後の行動に変化が見られた。これらの変化が胎仔・乳児が母体経由のBPA暴露を受けたことによるものか、あるいはBPA暴露に起因する母体の変化による副次的な影響なのか、更には別の未知の間接的な経路によるものなのか、現時点では判断できない。しかし、メカニズムが不明とは言え、胎生期および授乳期における母体のBPA暴露が仔の身体的発達および成長後の行動に影響を及ぼす危険性が否定できないので、本研究で得られた結果の再現性と妥当性について更なる検討が必要である。

雑誌

発表者氏名	論文タイトル名	発表誌名	巻号	ページ	出版年
Fujiki R, Hashiba W, Sekine H, Yokoyama A, Chikanishi T, Ito S, Imai Y, Kim J, He HH, Igarashi K, Kanno J, Ohtake F, Kitagawa H, Roeder RG, Brown M, Kato S.	GlcNAcylation of histone H2B facilitates its monoubiquitination.	Nature	480	557 – 561	2011
Matsukura H, Aisaki K, Igarashi K, Matsushima Y, Kanno J, Muramatsu M, Sudo K, Sato N.	Genistein promotes DNA demethylation of the steroidogenic factor 1 (SF-1) promoter in endometrial stromal cells.	Biochem Biophys Res Commun	412	366 – 372	2011
Baba A, Ohtake F, Okuno Y, Yokota K, Okada M, Imai Y, Ni M, Meyer CA, Igarashi K, Kanno J, Brown M, Kato S.	PKA-dependent regulation of the histone lysine demethylase complex PHF2-ARID5B.	Nat Cell Biol.	13	669 – 676	2011
Arase S, Ishii K, Igarashi K, Aisaki K, Yoshio Y, Matsushima A, Shimohigashi Y, Arima K, Kanno J, Sugimura Y.	Endocrine disrupter bisphenol A increases in situ estrogen production in the mouse urogenital sinus.	Biol Reprod.	84	734 – 742	2011
Higuchi, H., Iwano, H., Kawai, K., Ohta, T., Obayashi, T., Hirose, K., Itoh, N., Yokota, T., Tamura, Y. and Nagahata, H.	A simplified PCR assay for fast and easy mycoplasma mastitis screening in dairy cattle.	J. Vet. Sci.	12	191 – 193	2011

Higuchi, H., Iwano, H., Gondaira, S., Kawai, K., Nagahata, H.	Prevalence of Mycoplasma species in bulk tank milk in Japan.	Vet. Rec.	/	/	2011
Suzuki, K., Higuchi, H., Iwano, H., Lakritz, J., Sera, K., Koiwa, M., Taguchi, K.	Analysis of trace and major elements in bronchoalveolar lavage fluid of mycoplasma bronchopneumonia in calves.	Biol. Trace. Elem. Res.	145	166 – 171	2011
Sakurai M, Ohtake J, Ishikawa T, Tanemura K, Hoshino Y, Arima T, Sato E.	Distribution and Y397 phosphorylation of focal adhesion kinase on follicular development in the mouse ovary.	Cell Tissue Res.	347	457 – 465	2012
Hiradate Y, Ohtake J, Hoshino Y, Tanemura K, Sato E.	Adrenomedullin: a possible regulator of germinal vesicle breakdown.	Biochem Biophys Res Commun.	415	691 – 695	2011
Suh, J., Rivest, A.J., Nakashiba, T., Tominaga, T., and Tonegawa, S.	Entorhinal cortex layer III input to the hippocampus is crucial for temporal association memory.	*Science*	334	1415 – 1420	2011
Fujimoto Y., Abematsu M., Falk A., Tsujimura K., Sanosaka T., Juliandi B., Semi K., Namihira M., Komiya S., Smith A. and Nakashima K.	Treatment of a mouse model of spinal cord injury by transplantation of human iPS cell-derived long-term self-renewing neuroepithelial-like stem cells.	*Stem Cells*	/	/	in press

Mutoh T., Sanosaka T., Ito K. and Nakashima K.	Oxygen levels epigenetically regulate fate switching of neural precursor cells via HIF1α-Notch signal interaction in the developing brain.	*Stem Cells*	30	561 – 569	2012
Juliandi B., Abematsu M., Sanosaka T., Tsujimura K., Smith A. and Nakashima K.	Induction of superficial cortical layer neurons from mouse embryonic stem cells by valproic acid.	*Neurosci Res*	72	23 – 31	2012
Nagao H., Ijiri K., Hirotsu M., Ishidou Y., Yamamoto T., Nagano S., Takizawa T., Nakashima K., Komiya S. and Setoguchi T.	Role of GLI2 in the growth of human osteosarcoma.	*J Pathol*	224	169 – 179	2011
Kuwabara T., Kagalwala M.N., Onuma Y., Ito Y., Warashina M., Terashima K., Sanosaka T., Nakashima K., Gage F.H. and Asashima M.	Insulin biosynthesis in neuronal progenitors derived from adult hippocampus and the olfactory bulb.	*EMBO Mol Med*	3	742 – 754	2011
K. Yamada, C. Homma, K. Tanemura, T. Ikeda, S. Itohara, Y. Nagaoka	Analysis of fear memory in *Arc/Arg3.1*-deficient mice: intact short-term memory and impaired long-term and remote memory.	World Journal of Neuroscience	1	1 – 8	2011

M. Hatayama, A. Ishiguro, Y. Iwayama, T. Takashima, K. Sakoori, T. Toyota, Y. Nozaki, Y-S. Okada, K. Yamada, T. Yoshikawa, J. Aruga	Characterization of *Zic2* hypomorphic mutant mice as a schizophrenia model and *Zic2* mutation identified in schizophrenia patients.	Scientific Reports	1	1 – 11	2011
T. Saito, T. Suemoto, N. Mihira, Y. Matsuba, K. Yamada, P. Nilsson, J. Takano, M. Nishimura, N. Iwata, C. V. Broeckhoven, T. C. Saido	Potent in vivo amyloidogenicity of Aβ43.	Nature Neuroscience	14	1023 – 1032	2011
. Satoh, S. Endo, T. Nakata, Y. Kobayashi, K. Yamada, T. Ikeda, A. Takeuchi, T. Hiramoto, Y. Watanabe, T. Kazama	ERK2 Contributes to the Control of Social Behaviors in Mice.	Journal of Neuroscience	31	11953 – 11967	2011
N. Takashima, Y. S. Odaka, K. Sakoori, T. Akagi, T. Hashikawa, N. Morimura, K. Yamada, J. Aruga	Impaired cognitive function and altered hippocampal synapse morphology in mice lacking *Lrrtm1*, a gene associated with schizophrenia.	PLoS ONE	6	e22716	2011
T. Sano, Y-J. Kim, E. Oshima, C. Shimizu, Kiyonari. H, T. Abe, H. Higashi, K. Yamada, Y. Hirabayashi	Comparative characterization of GPRC5B and GPRC5C LacZ knockin mice; Behavioral abnormalities in GPRC5B-deficient mice.	Biochem Biophys Res Commun.	412	460 – 465	2011

LETTER

doi:10.1038/nature10656

GlcNAcylation of histone H2B facilitates its monoubiquitination

Ryoji Fujiki[1], Waka Hashiba[1], Hiroki Sekine[1], Atsushi Yokoyama[1], Toshihiro Chikanishi[1], Saya Ito[1], Yuuki Imai[1], Jaehoon Kim[2], Housheng Hansen He[3], Katsuhide Igarashi[4], Jun Kanno[4], Fumiaki Ohtake[1], Hirochika Kitagawa[1], Robert G. Roeder[2], Myles Brown[3] & Shigeaki Kato[1,5]

Chromatin reorganization is governed by multiple post-translational modifications of chromosomal proteins and DNA[1,2]. These histone modifications are reversible, dynamic events that can regulate DNA-driven cellular processes[3,4]. However, the molecular mechanisms that coordinate histone modification patterns remain largely unknown. In metazoans, reversible protein modification by *O*-linked *N*-acetylglucosamine (GlcNAc) is catalysed by two enzymes, *O*-GlcNAc transferase (OGT) and *O*-GlcNAcase (OGA)[5,6]. However, the significance of GlcNAcylation in chromatin reorganization remains elusive. Here we report that histone H2B is GlcNAcylated at residue S112 by OGT *in vitro* and in living cells. Histone GlcNAcylation fluctuated in response to extracellular glucose through the hexosamine biosynthesis pathway (HBP)[5,6]. H2B S112 GlcNAcylation promotes K120 monoubiquitination, in which the GlcNAc moiety can serve as an anchor for a histone H2B ubiquitin ligase. H2B S112 GlcNAc was localized to euchromatic areas on fly polytene chromosomes. In a genome-wide analysis, H2B S112 GlcNAcylation sites were observed widely distributed over chromosomes including transcribed gene loci, with some sites co-localizing with H2B K120 monoubiquitination. These findings suggest that H2B S112 GlcNAcylation is a histone modification that facilitates H2BK120 monoubiquitination, presumably for transcriptional activation.

Some nuclear proteins have been shown to be GlcNAcylated by OGT, for example the enzymatic activity of histone H3K4 methyltransferase 5 (MLL5) is modulated by GlcNAcylation[7–9]. To identify chromatin substrates for OGT further, we screened for unknown GlcNAcylated glycoproteins in HeLa cell chromatin. GlcNAcylated proteins were purified by WGA lectin column chromatography and anti-GlcNAc antibody (clone RL2). Liquid chromatography–mass spectrometry (LC–MS)/MS analysis of the fraction revealed 284 factors, including previously reported GlcNAcylated glycoproteins[6,10] (Supplementary Table 1). Among the candidates, the enrichment of nucleosomes was confirmed by silver staining and western blotting (Supplementary Fig. 2), suggesting one or more histone(s) might have been GlcNAcylated. As OGT is the only known nuclear enzyme for protein GlcNAcylation[5], we asked whether histones served as substrates for OGT *in vitro* (Supplementary Fig. 3). H2A and H2B, as well as H2A variants (H2A.X and H2A.Z), but not H3 and H4, appeared to be GlcNAcylated (Fig. 1a). With histone octamers, H2B, but not H2A, appeared to serve as a substrate (Fig. 1b). Likewise, H2B in *Drosophila* histone was also GlcNAcylated (Supplementary Fig. 4), implying that H2B GlcNAcylation is conserved in metazoans.

A quadrupole (Q)-time of flight (TOF) MS assessment of the *in vitro* GlcNAcylated H2B showed that OGT could transfer three GlcNAc moieties to H2B (Supplementary Fig. 5). Electro-transfer-dissociation (ETD)–MS/MS mapped the sites to S91, S112 and S123 (Fig. 1c and Supplementary Fig. 6). Unlike a recent report[11], we were unable to detect the reported sites in H2B S36 and H4 S47. However, H2A T101 was detected as a GlcNAc site when H2A protein alone was used (data not shown). This discrepancy in identified GlcNAc sites might be due to differences in experimental approaches.

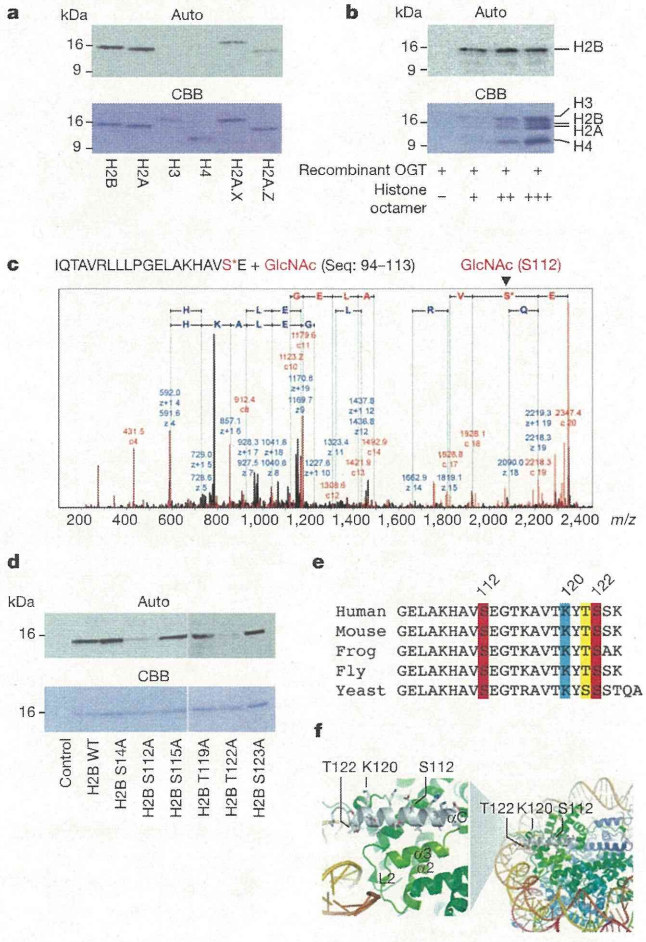

Figure 1 | H2B is GlcNAcylated at the C-terminal S112. a, **b**, *In vitro* OGT assay with recombinant histones (**a**) or the octamers reconstituted *in vitro* (**b**). Histones were GlcNAcylated by uridine diphosphate (UDP)-[^{3}H]GlcNAc and OGT, and the radiolabelled histones were subjected to autoradiography (top) and CBB staining (bottom). **c**, ETD–MS/MS scanned the GlcNAcylated peptides (2349.43 *m*/*z*) in Supplementary Fig. 5b. **d**, A series of H2B mutants at the indicated S/T was assessed by *in vitro* OGT assays. **e**, Sequence alignment of αC. **f**, The locations of the GlcNAc sites and the ubiquitination site of H2B in a nucleosome. The αC helix is illustrated as a white ribbon.

[1]Institute of Molecular and Cellular Biosciences, University of Tokyo, 1-1-1 Yayoi, Bunkyo-ku, Tokyo 113-0032, Japan. [2]Laboratory of Biochemistry and Molecular Biology, The Rockefeller University, New York, New York 10065, USA. [3]Department of Medical Oncology, Dana-Farber Cancer Institute and Harvard Medical School, Boston, Massachusetts 02115, USA. [4]Division of Cellular and Molecular Toxicology, National Institute of Health Sciences, 1-18-1 Kamiyoga, Setagaya-ku, Tokyo 158-8501, Japan. [5]ERATO, Japan Science and Technology Agency, Kawaguchi, Saitama 332-0012, Japan.

Next, *in vitro* OGT assays using peptide arrays covering full-length H2B revealed peaks at 101–115 peptides in the carboxy (C)-terminal α-helix (αC)[12] (Supplementary Fig. 7). This peptide was found to bear only one moiety by matrix-assisted laser desorption/ionization–time of flight (MALDI–TOF)/MS (Supplementary Fig. 8). Indeed, substitutions of S112 and T122 to A significantly reduced *in vitro* GlcNAcylation by OGT (Fig. 1d), but not mutations in the amino (N)-terminal tail (Supplementary Fig. 9). On the basis of these data, we concluded that the conserved S112 was a GlcNAc site in H2B, whereas T122 might be needed for recognition by OGT (Fig. 1e, f).

With our newly developed antibody (Supplementary Fig. 10), H2B S112 GlcNAc was detected in histones of HeLa cells. Depletion of glucose from the media for 24 h induced deglycosylation with neither overt cell death (Fig. 2a and Supplementary Fig. 11) nor alteration in histone acetylation marks of cell state indicators (H3 K14, H3 K56, H4 K16)[13,14] (Supplementary Fig. 12). H2B S112 GlcNAc could be restored by re-treatment with glucose at physiological concentrations (Supplementary Fig. 13).

Because many histone modifications are orchestrated, we tested if H2B S112 GlcNAc influenced H2B K120 monoubiquitination because of their proximity. After glucose depletion, replenishment of glucose gradually increased global GlcNAcylation of proteins, followed by H2B S112 GlcNAc and H2B monoubiquitination (Fig. 2b, c). Their reciprocal modifications disappeared when OGT was knocked down (Fig. 2d and Supplementary Fig. 14). In addition, in the immunoprecipitates of H2B containing the S112A and T122A double mutations (H2B AA), no response of K120 monoubiquitination to extracellular glucose was detected (Fig. 2e and Supplementary Fig. 15). Conversely, GlcNAcylation of H2B S112 was observed, even when K120 was mutated to R (Fig. 2e). From these findings, we conclude that H2B K120 monoubiquitination is mediated, at least in part, through S112 GlcNAcylation.

As glucosamine, but not pyruvate, potentiated H2B S112 GlcNAc (Fig. 2f), it appeared that this GlcNAcylation step was dependent on the HBP. To clarify this point, two HBP inhibitors (DON and AZA) were tested (Supplementary Information). After glucose depletion from media, these inhibitors attenuated the effect of glucose in H2B S112 GlcNAcylation along with K120 monoubiquitination (Fig. 2f).

In yeast, it was previously shown that H2B K120 monoubiquitination was induced by carbohydrates by glycolysis[15]. To address this issue, inhibitors of both glycolysis and deGlcNAcylation were applied to assess the crosstalk between the two modifications. When the cells were treated with iodoacetate, which blocks glycolysis but not HBP[15], the glucose effects on histone modifications were impaired, whereas the additional treatment of an OGA inhibitor (PUGNAc) restored both H2B S112 and K120 monoubiquitination (Supplementary Fig. 16). These data support the notion that H2B S112 GlcNAc senses decreases in glucose levels below normal levels and acts to promote H2B monoubiquitination, a modification that is associated with active transcription. Together with the fact that OGT is absent in yeast[6], the present H2B S112 GlcNAc-dependent pathway appears to constitute a system capable of sensing nutritional states in metazoans.

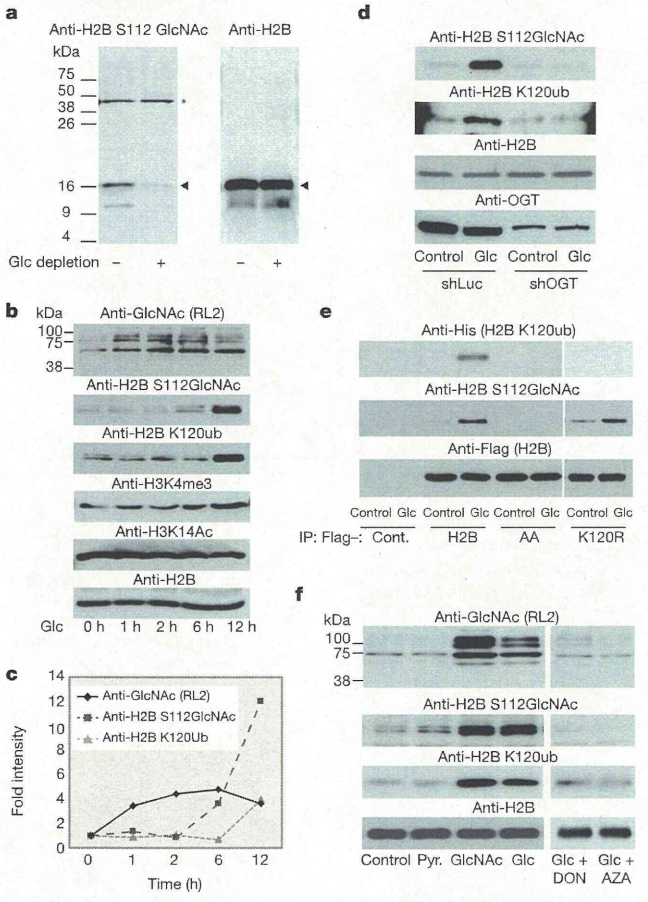

Figure 2 | H2B S112 GlcNAc is a glucose-responsive modification linked to K120 monoubiquitination (ub). **a**, Chromatin was prepared from HeLa cells cultured in media with or without 1 g l^{-1} glucose (Glc) for 24 h, and subjected to western blotting. Arrowheads show the indicated proteins. Asterisks indicate non-specific band. **b**, **c**, After 24 h Glc depletion, chromatin samples were prepared from HeLa cells treated with 4.5 g l^{-1} Glc for the indicated time. The intensities of the western blotting bands (**b**) were quantified (**c**). **d**, **e**, The effects of OGT knockdown (**d**) or H2B mutations (**e**) on H2B modifications after Glc replenishment. **f**, Western blotting analysis of the H2B modifications in HeLa cells that were cultured in DMEM without Glc (Cont.), or supplemented with 1 mM pyruvate (Pyr.), 10 mM GlcNAc or 4.5 g l^{-1} Glc with or without HBP inhibitors, 6-diazo-5-oxo-L-norleucine (100 μM, DON) or azaserine (100 μM, AZA).

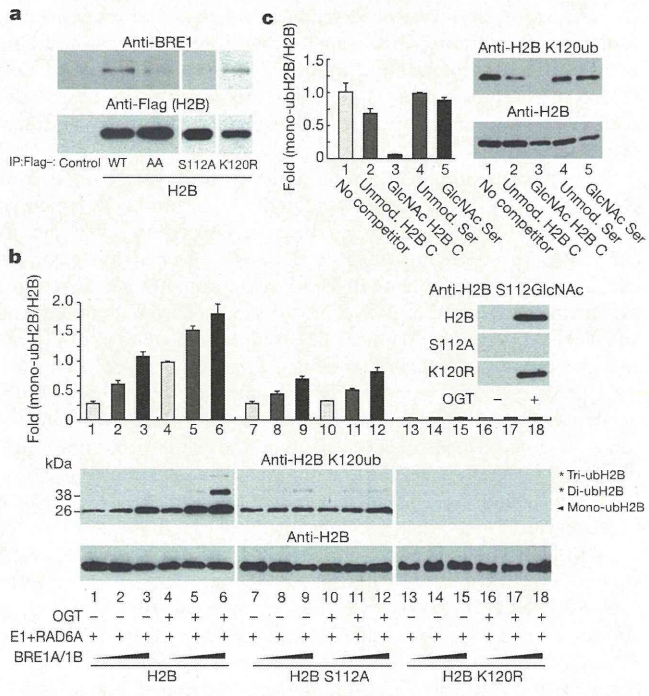

Figure 3 | GlcNAcylation at S112 facilitates ubiquitination at K120 in H2B. **a**, Western blotting analysis of the interaction of H2B mutants with BRE1A. **b**, **c**, *In vitro* monoubiquitination assay with GlcNAcylated H2B (**b**), or in the presence of competitor peptides (**c**). H2B was GlcNAcylated *in vitro* (**b**, top right), and the reactants were subsequently ubiquitinated by H2B monoubiquitination ligase. The reaction was performed with the indicated competitor peptides (0.25 μg ml^{-1}) (**c**). H2B K120 monoubiquitination was detected by western blotting (**b**, bottom; **c**, right) and quantified (**b**, top; **c**, left). Error bars, means and s.d. ($n = 3$).

The terminal GlcNAc of polysaccharides reportedly serves as a recognition moiety for E3 monoubiquitination ligase[16]. Therefore, we proposed that H2B S112 GlcNAc affected K120 monoubiquitination by the BRE1A/1B complex[17]. Flag-tagged H2B, but not AA or S112A, was co-immunoprecipitated with BRE1A (Fig. 3a). This association was observed in the presence of physiological levels of glucose in the media, and BRE1A was bound to H2B S112 GlcNAc (Supplementary Fig. 17). We then assessed how the GlcNAcylation of H2B influenced its *in vitro* ubiquitination by E1, RAD6A (E2) and the BRE1A/1B complex (E3). Although H2B K120 could be substantially ubiquitinated only by the ligases (Supplementary Fig. 18), GlcNAcylation of H2B promoted subsequent H2B ubiquitination, but not its S112A mutant (Fig. 3b). Likewise, ubiquitination was significantly attenuated by the presence of an H2B-S112-GlcNAcylated peptide, but not by either the unmodified control peptide or by GlcNAcylated serine (Fig. 3c). On the basis of these results, we conclude that the GlcNAc moiety at H2B S112 may anchor H2B monoubiquitination ligase.

To illustrate the role of H2B S112 GlcNAc in chromatin regulation, its location was visualized on fly polytene chromosomes. H2B S112 GlcNAc was detected widely in euchromatin, and, as anticipated, its signal disappeared in an OGT-disrupted fly, sxc^{1}/sxc^{78} (Supplementary Fig. 19). H2B S112 GlcNAc overlapped with H3K4 me2 more than with H3K9 me2 or H3K27 me3 (Fig. 4a). Similarly, in immunostained HeLa cells, H2B S112 GlcNAc sites appeared exclusively in 4′,6-diamidino-2-phenylindole (DAPI)-poor areas (Supplementary Fig. 20). Thus, H2B S112 GlcNAc probably accumulates in active chromatin rather than inactive chromatin.

To determine the precise loci of H2B S112 GlcNAc in HeLa cells, we performed chromatin immunoprecipitation (ChIP) and high-throughput sequencing (ChIP-seq). We confirmed ChIP quality by enrichments of H2B GlcNAc as well as H3K4 me2 and H2B K120 monoubiquitination, but neither H3K9 me2 nor H3K27 me3 (Supplementary Fig. 21). A total of 47,375 peaks were found widely distributed over the genome (Supplementary Fig. 22). However, H2B S112 GlcNAc peaked near transcription start sites (TSS), whereas the distribution decreased at transcription termination sites (TTS) (Fig. 4b), suggesting that it correlated with transcriptional regulation. To test this assumption, the activities of genes harbouring H2B S112 GlcNAc near TSS were estimated by microarray analysis (Supplementary Table 2). The average profiles near TSS significantly correlated with gene activity (Fig. 4c). Moreover, the expression levels of the 1,299 genes were reliably measured, and 1,021 genes showed high expression (Supplementary Fig. 23a and Supplementary Table 3b). Moreover, gene ontology analysis revealed that there was an association of the genes harbouring H2B S112 GlcNAc to cellular metabolic processes (Supplementary Fig. 23b and Supplementary Table 3c).

Next, we analysed the genome-wide overlap of H2B S112 GlcNAc with K120 monoubiquitination. A total of 44,158 peaks of H2B K120 monoubiquitination were detected, and their average profiles near TSS were similar to those profiles of H2B S112 GlcNAc (Supplementary

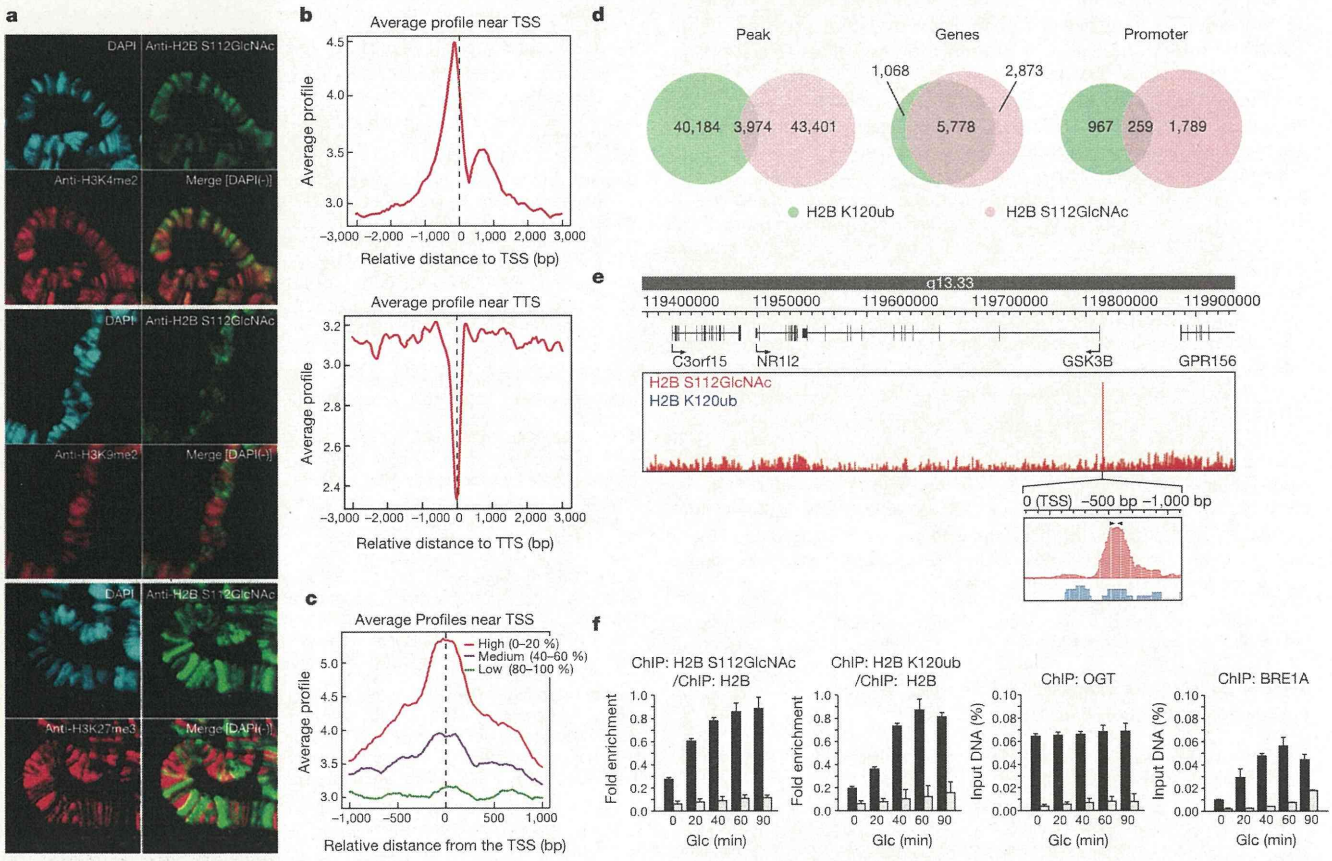

Figure 4 | GlcNAcylated H2B is associated with transcribed genes. **a**, Polytene staining with α-H2B S112 GlcNAc (green) and DAPI (blue) along with α-H3K4me2 (red, top), α-H3K9me2 (red, middle) or α-H3K27me3 (red, bottom). **b**–**e**, ChIP-seq analysis of the H2B S112 GlcNAc and K120 monoubiquitination. The distributions of H2B S112 GlcNAc were averaged near TSS (top) and TTS (bottom) (**b**). The average profiles of H2B S112 GlcNAc near TSS were calculated based on the associated gene activities (**c**). Venn diagrams showing overlap of the peaks (**d**, left), and the genes (**d**, middle) and the promoter (**d**, right) harbouring the modifications. The ChIP-seq profile surrounding the *GSK3B* gene (**e**). Arrowhead, position of qPCR primer. **f**, ChIP–qPCR validation in the GSK3B promoter. After Glc depletion, the control HeLa cells (black bar) and the OGT-knockdown cells (white bar) were replenished with Glc for 24 h. Then, the cells were subjected to ChIP with the indicated antibody and qPCR analysis. Error bars, means and s.d. ($n = 3$).

Fig. 24). Among the H2B K120 monoubiquitination peaks, nearly 10% (3,974 peaks) overlapped with H2B S112 GlcNAc peaks (Fig. 4d, left), and this evaluation was confirmed by a sequential ChIP–reChIP assay (Supplementary Fig. 25). Although 5,778 genes (66.8% of H2B S112 GlcNAc and 84.4% of K120 monoubiquitination) were found at the same loci (Fig. 4d, middle, and Supplementary Table 3d), 259 genes were identified when the two peaks were compared only within the promoters (Fig. 4d, right). The results of the ChIP-seq analysis were validated by ChIP–quantitative PCR (qPCR) assessment for the glycogen synthase kinase 3β (*GSK3B*) gene (Fig. 4e, f). These findings suggest that at several H2B S112 GlcNAc sites, it aids H2B monoubiquitination ligase recruitment whereas at others additional or different factors may be operational.

Here we provide evidence that histone GlcNAcylation is a post-translational modification correlated with active transcriptional events, and is responsive to serum glucose levels and/or cellular energy states in certain cell types (Supplementary Fig. 1). Using an antibody that specifically recognizes the S112 GlcNAc moiety of endogenous H2B, H2B was shown to serve as an OGT substrate. We have focused on the role of H2B S112 GlcNAcylation in gene regulation (Supplementary Fig. 1). Genome-wide analysis revealed that H2B S112 GlcNAc was frequently located near transcribed genes, suggesting that histone GlcNAcylation facilitates transcription of the genes. This idea is supported by previous reports that transcriptional output driven by several transcription factors is co-activated by OGT[9,18–20]. However, recent papers reported that *Drosophila* OGT is itself a polycomb group protein[8,21], and that many *O*-GlcNAcylated factors are involved in transcriptional repression and gene silencing[7,8]. In this respect, it will be interesting to identify other histone glycosylation sites and investigate their roles in transcriptional repression as well as activation.

METHODS SUMMARY

Plasmids and cell culture. All plasmids were generated with standard protocols (see Methods). Retrovirus production, infection and sorting of the infected cells followed previously reported protocols[9].

Purification of GlcNAc proteins from chromatin. Chromatin pellets were prepared from HeLa cells as previously described[22]. GlcNAc proteins were enriched with α-*O*-GlcNAc (RL2) antibody (Abcam) immobilized on Dynabeads (Invitrogen), and released with GlcNAc-*O*-serine.

Generation of monoclonal antibody. The synthetic H2B S112 GlcNAc peptide (CKHAV S(GlcNAc) EGTK) was used to immunize mice. The hybridomas were selected by enzyme-linked immunosorbent assay (ELISA) and western blotting analysis.

***In vitro* OGT and monoubiquitination assays.** Flag–OGT, Flag–E1, and Flag–BRE1A/BRE1B were purified by baculoviral systems, whereas histones and 6 × His-RAD6A were prepared from bacteria as previously reported[17,23]. H2B was incubated with OGT or H2B monoubiquitination ligases *in vitro*, and its modification was detected by western blotting as previously reported[9,23].

ChIP-seq and ChIP–qPCR. ChIP and ChIP-seq library construction was performed as previously described[24,25], and the libraries were sequenced to 50 base pairs (bp) with Hiseq2000 (Illumina). The fragments of interest in the libraries were quantified with specific promoter sets (Methods) by qPCR.

Full Methods and any associated references are available in the online version of the paper at www.nature.com/nature.

Received 16 July 2010; accepted 20 October 2011.
Published online 27 November 2011.

1. Strahl, B. D. & Allis, C. D. The language of covalent histone modifications. *Nature* **403,** 41–45 (2000).
2. Kouzarides, T. Chromatin modifications and their function. *Cell* **128,** 693–705 (2007).
3. Li, B., Carey, M. & Workman, J. L. The role of chromatin during transcription. *Cell* **128,** 707–719 (2007).
4. Berger, S. L. The complex language of chromatin regulation during transcription. *Nature* **447,** 407–412 (2007).
5. Hart, G. W., Housley, M. P. & Slawson, C. Cycling of O-linked β-*N*-acetylglucosamine on nucleocytoplasmic proteins. *Nature* **446,** 1017–1022 (2007).
6. Love, D. C. & Hanover, J. A. The hexosamine signaling pathway: deciphering the 'O-GlcNAc code'. *Sci. STKE* **2005,** re13 (2005).
7. Yang, X., Zhang, F. & Kudlow, J. E. Recruitment of O-GlcNAc transferase to promoters by corepressor mSin3A: coupling protein O-GlcNAcylation to transcriptional repression. *Cell* **110,** 69–80 (2002).
8. Gambetta, M. C., Oktaba, K. & Muller, J. Essential role of the glycosyltransferase sxc/Ogt in polycomb repression. *Science* **325,** 93–96 (2009).
9. Fujiki, R. *et al.* GlcNAcylation of a histone methyltransferase in retinoic-acid-induced granulopoiesis. *Nature* **459,** 455–459 (2009).
10. Wang, Z. *et al.* Extensive crosstalk between O-GlcNAcylation and phosphorylation regulates cytokinesis. *Sci. Signal.* **3,** ra2 (2010).
11. Sakabe, K., Wang, Z. & Hart, G. W. β-N-acetylglucosamine (O-GlcNAc) is part of the histone code. *Proc. Natl Acad. Sci. USA* **107,** 19915–19920 (2010).
12. Luger, K. *et al.* Crystal structure of the nucleosome core particle at 2.8 Å resolution. *Nature* **389,** 251–260 (1997).
13. Das, C., Lucia, M. S., Hansen, K. C. & Tyler, J. K. CBP/p300-mediated acetylation of histone H3 on lysine 56. *Nature* **459,** 113–117 (2009).
14. Dang, W. *et al.* Histone H4 lysine 16 acetylation regulates cellular lifespan. *Nature* **459,** 802–807 (2009).
15. Dong, L. & Xu, C. W. Carbohydrates induce mono-ubiquitination of H2B in yeast. *J. Biol. Chem.* **279,** 1577–1580 (2004).
16. Yoshida, Y. *et al.* E3 ubiquitin ligase that recognizes sugar chains. *Nature* **418,** 438–442 (2002).
17. Kim, J. *et al.* RAD6-Mediated transcription-coupled H2B ubiquitylation directly stimulates H3K4 methylation in human cells. *Cell* **137,** 459–471 (2009).
18. Dentin, R. *et al.* Hepatic glucose sensing via the CREB coactivator CRTC2. *Science* **319,** 1402–1405 (2008).
19. Chikanishi, T. *et al.* Glucose-induced expression of MIP-1 genes requires O-GlcNAc transferase in monocytes. *Biochem. Biophys. Res. Commun.* **394,** 865–870 (2010).
20. Jackson, S. P. & Tjian, R. O-glycosylation of eukaryotic transcription factors: implications for mechanisms of transcriptional regulation. *Cell* **55,** 125–133 (1988).
21. Sinclair, D. A. *et al. Drosophila* O-GlcNAc transferase (OGT) is encoded by the Polycomb group (PcG) gene, super sex combs (sxc). *Proc. Natl Acad. Sci. USA* **106,** 13427–13432 (2009).
22. Sawatsubashi, S. *et al.* A histone chaperone, DEK, transcriptionally coactivates a nuclear receptor. *Genes Dev.* **24,** 159–170 (2009).
23. Fujiki, R. *et al.* Ligand-induced transrepression by VDR through association of WSTF with acetylated histones. *EMBO J.* **24,** 3881–3894 (2005).
24. He, H. H. *et al.* Nucleosome dynamics define transcriptional enhancers. *Nature Genet.* **42,** 343–347 (2010).
25. Minsky, N. *et al.* Monoubiquitinated H2B is associated with the transcribed region of highly expressed genes in human cells. *Nature Cell Biol.* **10,** 483–488 (2008).

Supplementary Information is linked to the online version of the paper at www.nature.com/nature.

Acknowledgements We thank A. Miyajima, S. Saito and N. Moriyama for experimental support, and M. Yamaki for manuscript preparation. We also thank Y. Maekawa, J. Seta and N. Iwasaki for support with MS. This work was supported in part by The Naito Foundation, the Astellas foundation (to R.F.), the Ministry of Education, Culture, Sports, Science and Technology (MEXT) and the Japan Society for the Promotion of Science (to R.F. and S.K.).

Author Contributions S.K. planned the study with H.K.; R.G.R. and M.B. provided support and general guidance; R.F. designed the study and performed the experiments with H.S. (α-*O*-GlcNAc purification), A.Y. (LC–MS/MS), W.H. (*O*-GlcNAc site mapping), T.C. (*in vitro* OGT assay), S.I. (*Drosophila* analysis), Y.I., H.H.H. (ChIP-seq), F.O., J.K. (*in vitro* monoubiquitination assay), K.I. and J.K (microarray).

Author Information Reprints and permissions information is available at www.nature.com/reprints. The authors declare no competing financial interests. Readers are welcome to comment on the online version of this article at www.nature.com/nature. Correspondence and requests for materials should be addressed to S.K. (uskato@mail.ecc.u-tokyo.ac.jp).

METHODS

Plasmids and retroviruses. Complementary DNAs (cDNAs) of N-terminally Flag-tagged H2B and its mutant were subcloned into pcDNA3 (Invitrogen). A series of H2B point mutants were subcloned into the pET3 vector (Novagen). shRNA sequences targeting hOGT (5′-GCACATAGCAATCTGGCTTCC-3′) and *Renilla* luciferase (5′-TGCGTTGCTAGTACCAAC-3′, as a control) were inserted into the pSIREN-RetroQ-ZsGreen vector (Clontech). For retroviral production, the constructed shRNA vectors were transfected into PLAT-A cells. The virus contained in the medium was used for infection.

Generation of stable cell lines. To generate OGT-KD cells by retroviral infection, 10^6 cells were plated in 60 mm culture dishes, treated with 3 ml of retroviral cocktail (1 ml of the prepared retroviral solution plus 2 ml of DMEM with 10% FBS and 8 μg ml^{-1} polybrene), then cultured for another 48 h. A FACSVantage (BD) sorter was used to isolate the retrovirally transduced, enhanced green fluorescent protein (eGFP)-positive cells, as previously described[9]. To generate the cells stably expressing Flag-tagged constructs, HeLa cells were transfected with the pcDNA vectors encoding the Flag-tagged H2B or the AA mutant. The cells containing the integrated vectors were selected by exposure to 0.5 mg ml^{-1} G418.

Generation of monoclonal antibody. H2B S112 GlcNAc peptide (CKHAV S(GlcNAc) EGTK) was synthesized (MBL Institute) and used as an antigen (Operon Biotechnologies). The hybridomas were briefly screened using ELISA with the GlcNAc peptide, and finally selected by immunoblot analysis with the *in vitro* GlcNAcylated H2B.

Antibodies. Antibodies were obtained as follows: α-Flag M2 agarose (Sigma), α-H2A, α-H2B, α-H3, α-H4 (Abcam), α-H2B K120 monoubiquitination (Upstate), α-GlcNAc (RL2 or CTD110.6) (Abcam), α-OGT (Sigma), α-Flag (Sigma) and α-RNF20/BRE1A (Bethyl).

Purification and identification of GlcNAc proteins. The α-*O*-GlcNAc-immobilized beads were prepared with 15 μg α-*O*-GlcNAc (RL2) antibody and 0.5 ml of Dynabeads M-280 sheep α-mouse IgG (Invitrogen) according to the manufacturer's instructions. Chromatin extracts from HeLa cells (0.5 g protein) were prepared essentially as previously described[22]. In brief, the chromatin pellet, which consisted of residual material from the nuclear extract preparation with buffers supplemented with 1 mM streptozotocin (STZ), was re-suspended with micrococcal nuclease (MNase) buffer (20 mM Tris-HCl, 1 mM $CaCl_2$, 2 mM $MgCl_2$, 0.1 M KCl, 0.1% (v/v) Triton-X, 0.3 M sucrose, 1 mM DTT, 1 mM benzamidine, 0.2 mM PMSF, 1 mM STZ, pH 7.9). After addition of 3 U ml^{-1} MNase, the samples were incubated for 30 min at room temperature with continuous homogenization and the reaction was stopped by adding 5 mM EGTA and 5 mM EDTA. After centrifugation at 2,000*g* for 30 min at 4 °C, the supernatant (chromatin extract) was used for the following purification steps. The chromatin extracts were passed through a WGA agarose column (Vector). The flow-through fraction was further mixed with α-*O*-GlcNAc-immobilized beads and rotated for 8 h at 4 °C. After three washes with buffer D (20 mM Tris-HCl, 0.2 mM EDTA, 5 mM $MgCl_2$, 0.1 M KCl, 0.05% (v/v) NP-40, 10% (v/v) glycerol, 1 mM DTT, 1 mM benzamidine, 0.2 mM PMSF, 1 mM STZ, pH 7.9), glycoproteins were eluted twice with buffer D plus 0.4 mg ml^{-1} GlcNAc-*O*-serine (MBL) (elutions 1 and 2) and finally with 0.1 M glycine-HCl (pH2.0) (elution 3). Eluted proteins were desalted by methanol–chloroform precipitation, digested with trypsin (Promega) then loaded on the automated LC–MS/MS system, which was assembled with Zaplous nano-LC (AMR) plumbed with a reverse-phase C18 electrospray ionization (ESI) column (LC assist) and a Fiinigan LTQ ion-trap mass spectrometer (Thermo). The LC–MS/MS data were processed using Thermo BioWorks (Thermo) and SEQUEST (Thermo) for protein identification. The list of the identified proteins was further analysed by using the 'gene functional classification tool' in DAVID bioinformatics resources 6.7 (http://david.abcc.ncifcrf.gov/).

Recombinant proteins. Preparation of recombinant proteins was performed as previously reported[9,23]. Recombinant Flag–OGT, Flag–E1, Flag–BRE1A/B complexes were isolated by baculovirus expression and immunoprecipitation-based purification with α-Flag M2 agarose (Sigma). Recombinant 6 × His-RAD6A was expressed in bacteria and partly isolated with a HIS-Select Nickel Affinity Gel (Sigma). The eluate was diluted 1:20 with BC0 (20 mM HEPES, 0.2 mM EDTA, 10% (v/v) glycerol, pH 7.9), and fractionated with a Resource Q column (GE Healthcare) using a linear gradient (0–0.5 M KCl) method. Preparation of recombinant *Xenopus* histone H2B and its mutants was performed as previously described[9,23].

***In vitro* GlcNAcylation assay (autoradiographic analysis).** Recombinant Flag–OGT protein (0.5 μg) was incubated with 0.5 μg of recombinant histone and 0.2 mM (0.2 μCi) UDP-[^{3}H]GlcNAc (PerkinElmer) in a 25 μl reaction (50 mM Tris-HCl, 12.5 mM $MgCl_2$, 1 mM DTT, pH 7.5) for 24 h at 37 °C. The reaction was resolved with SDS–PAGE, blotted onto a polyvinylidene difluoride (PVDF) membrane, then subjected to autoradiography after spraying EN^{3}HANCE (NEN Lifescience).

***In vitro* GlcNAcylation assay (MS analysis).** Recombinant histones (1 μg) or recombinant histone octamers assembled *in vitro* (1 μg) were GlcNAcylated by recombinant Flag–OGT in 25 μl reactions (50 mM Tris-HCl, 2 mM UDP-GlcNAc, 12.5 mM $MgCl_2$, 1 mM DTT, pH 7.5) for 24 h at 37 °C. The reactions were directly subjected to a nano-LC ESI–TOF mass spectrometer system, which was assembled with a 1100 nanoLC (Agilent) plumbed with a ZORBAX 300SB-C18 column (Agilent) and micrOTOF (Bruker). Or, the reactions were digested with trypsin (Promega) and subjected to purification of glycopeptides with an MB-LAC WGA kit (Bruker). The enriched glycopeptides were loaded on the nano-LC ESI–ETD ion-trap mass-spectrometer system, which was assembled with the Agilent HP1200 Nano (Agilent) plumbed with ZORBAX 300SB-C18 (Agilent) and amaZon ETD (Bruker).

***In vitro* monoubiquitination assay.** GlcNAcylated histones (1 μg) were ubiquitinated with the E1 (0.1 μg), RAD6 (0.2 μg), BRE1 complex (0.5 μg), ubiquitin (3 μg) in 50 mM Tris (pH7.9), 5 mM $MgCl_2$, 4 mM ATP at 37 °C for 24 h.

ChIP-seq and ChIP–qPCR. ChIP and ChIP-seq libraries were constructed as previously described[24,25]. For ChIP-seq analysis, the libraries were sequenced to 50 bp with Hiseq2000 (Illumina). For ChIP–qPCR analysis, the fragments of interest in the libraries were quantified with Thermal Cycler TP800 (TAKARA) and SYBR Premix Ex Taq II (Takara). The qPCR primer sets for the *GSK3B* gene were 5′-TGCAAGCTCTCAGACGCTAA-3′ and 5′-CTCATTTCTCATGGGCG TTT-3′.

Biochemical and Biophysical Research Communications 412 (2011) 366–372

Contents lists available at ScienceDirect

Biochemical and Biophysical Research Communications

journal homepage: www.elsevier.com/locate/ybbrc

Genistein promotes DNA demethylation of the steroidogenic factor 1 (SF-1) promoter in endometrial stromal cells

Hiroshi Matsukura [a], Ken-ichi Aisaki [b], Katsuhide Igarashi [b], Yuko Matsushima [b], Jun Kanno [b], Masaaki Muramatsu [a], Katsuko Sudo [a,c], Noriko Sato [a,*]

[a] Department of Molecular Epidemiology, Medical Research Institute, Tokyo Medical and Dental University, 2-3-10 Kanda-surugadai, Chiyoda-ku, Tokyo 101-0062, Japan
[b] Division of Cellular and Molecular Toxicology, National Institute of Health Sciences, 1-18-1 Kamiyoga, Setagaya-ku, Tokyo 158-8501, Japan
[c] Animal Research Center, Tokyo Medical University, 6-1-1 Shinjuku, Shinjuku-ku, Tokyo 160-8402, Japan

ARTICLE INFO

Article history:
Received 21 July 2011
Available online 29 July 2011

Keywords:
Genistein
DNA methylation
Ovariectomized mice
Primary culture
Steroidogenic factor 1
High-resolution melting analysis

ABSTRACT

It has recently been demonstrated that genistein (GEN), a phytoestrogen in soy products, is an epigenetic modulator in various types of cells; but its effect on endometrium has not yet been determined. We investigated the effects of GEN on mouse uterine cells, *in vivo* and *in vitro*. Oral administration of GEN for 1 week induced mild proliferation of the endometrium in ovariectomized (OVX) mice, which was accompanied by the induction of steroidogenic factor 1 (SF-1) gene expression. GEN administration induced demethylation of multiple CpG sites in the SF-1 promoter; these sites are extensively methylated and thus silenced in normal endometrium. The GEN-mediated promoter demethylation occurred predominantly on the luminal side, as opposed to myometrium side, indicating that the epigenetic change was mainly shown in regenerated cells. Primary cultures of endometrial stromal cell colonies were screened for GEN-mediated alterations of DNA methylation by a high-resolution melting (HRM) method. One out of 20 colony-forming cell clones showed GEN-induced demethylation of SF-1. This clone exhibited a high proliferation capacity with continuous colony formation activity through multiple serial clonings. We propose that only a portion of endometrial cells are capable of receiving epigenetic modulation by GEN.

1. Introduction

Genistein (GEN), a major phytoestrogen in dietary soy, is a substantial component of the typical Asian and Western vegetarian diets, as well as recently developed infant soy milk formulas. There are several well known potential health benefits of GEN intake [1,2], one of which is an apparent decreased risk of breast and prostate cancers, based on human observational studies [1,3]. But GEN also paradoxically stimulates growth of breast cancer cells in culture [2] and uterine enlargement in rodents [4]. These effects may be mediated through estrogen receptor interactions and/or modulation of endogenous estrogen metabolism [5,6]. Since GEN can bind to estrogen receptors (ERs) α and β, with a stronger affinity to ERβ [5], it is categorized as a phyto-selective estrogen receptor modulator (SERM) [6,7]. The variations in GEN's agonistic or antagonistic effects may be affected by variations in endogenous estrogen levels. Previous studies have not determined whether the pleiotropic effects of GEN involve distinct epigenetic alteration. Recently, GEN was shown to alter DNA methylation in various types of cells, including ES cells [8], but most studies have been performed using cancer cell lines [9–11]. There have been few reports of the effects of GEN on DNA methylation in intact cells or *in vivo* [12]. In the present study, we utilized a uterotropic assay in ovariectomized (OVX) mice, as a model system to analyze epigenetic regulation by GEN.

In a previous study, high-dose GEN administration to OVX rats resulted in increased uterine weight and changed endometrial cell gene expression [6]. However, no epigenetic alterations were demonstrated under this condition. We selected the steroidogenic factor 1 (SF-1; official symbol: Nr5a1) gene as a target for the methylation analysis. SF-1 is an orphan nuclear receptor and transcription factor for key enzymes involved in steroidogenesis, such as StAR, Cyp11a1 (p450scc), Cyp17a1 (p450c17), and Cyp19a1 (aromatase) [13]. The SF-1 gene is not expressed in normal endometrium; however, SF-1 expression is reactivated in the disease state of human ectopic endometriosis, in which the SF-1 promoter is abnormally demethylated by an unknown mechanism [14]. The subsequent enhancement of steroidogenic genes and resultant local steroidogenesis are proposed to be important etiologies [15]. Therefore, we hypothesized that in mouse endometrial cells,

* Corresponding author. Fax: +81 3 5280 8058.
E-mail addresses: hmatsukura.epi@mri.tmd.ac.jp (Hiroshi Matsukura), nsato.epi@tmd.ac.jp (N. Sato).

0006-291X/$ - see front matter © 2011 Elsevier Inc. All rights reserved.
doi:10.1016/j.bbrc.2011.07.104

SF-1 might be subjected to epigenetic modulation by some external stimuli. Here we show that the SF-1 promoter was demethylated *in vivo* and *in vitro* by GEN treatment. This is the first demonstration of a phytoestrogen altering the epigenetic state of adult endometrium.

2. Materials and methods

2.1. Ethics statement

All procedures described here were performed according to protocols approved by the Animal Care Committee of the National Institute of Health Sciences, and Tokyo Medical and Dental University (No. 0110306A).

2.2. Oral administration of genistein to ovariectomized mice

C57BL/6JJmsSlc female mice (SLC) were used in this study. All mice were fed a phytoestrogen-free diet (Oriental Yeast) and were ovariectomized (OVX) 2 weeks prior to the genistein (GEN) treatment. OVX mice were divided into three different treatment groups, each consisting of 3–5 independent replicates, which orally received low-dose GEN (60 mg/kg/day), high-dose GEN (200 mg/kg/day), or vehicle (0.5% CMC-Na (Maruishi Pharmaceutical); 5 ml/kg/day) for 1 week. At the end of treatment (9 weeks of age), all mice were euthanized by exsanguination under ether anesthesia.

2.3. Uterotrophic assay and gene expression study after oral administration of genistein

Whole uteri were harvested, blotted, and weighted. Each uterus was divided into two horns, immediately placed into 2 ml plastic tubes of RNAlater solution (Ambion), and stored at 4 °C. From each sample, one horn was processed for mRNA expression analyses; RNAlater was replaced with 1.0 ml of RLT buffer (Qiagen), and the horn was homogenized by addition of a 5 mm diameter Zirconium bead (Funakoshi) and shaking with a MixerMill 300 (Qiagen) at 20 Hz for 5 min (only the outermost row of the shaker box was used). Further sample preparation and analysis were performed as previously described [16]. mRNA expressions were analyzed using Affymetrix Murine Genome 430 2.0 GeneChips, and calculated as copy number per cell by the Percellome method [16]. The second uterine horn of each sample was subjected to genomic DNA isolation.

2.4. Isolation of colony-forming cells derived from intact uteri

Five 8- to 9-week-old C57BL/6JJmsSlc female mice (SLC) were euthanized by cervical dislocation and whole uteri were harvested. Uterine horns were collected in Dulbecco's modified Eagle's medium/Hams F-12 (DMEM/F-12; Nacalai Tesque) containing 0.05 mg/ml gentamicin (Sigma–Aldrich). Each horn was dissected longitudinally and the endometrial tissue was divided into two portions: the luminal side and the myometrium side. A single cell suspension of endometrial cells was obtained using enzymatic digestion and mechanical means adapted from Chan et al. [17]. The tissue samples were minced and dissociated in 500 μl DMEM/F-12 containing 0.12 mg/ml (0.56 Wünsch U/ml) Blendzyme 2 and 40 μg/ml deoxyribonuclease type I (both from Roche Applied Science) in a shaking incubator (~90 rpm) at 37 °C. At 15 min intervals, the digests were pipetted to promote separation and cell dissociation was monitored microscopically. After 45 min, debris was filtered out using a 40-μm sieve (BD Biosciences). The single-cell suspensions were collected in DMEM/F-12 containing 10% FBS, 0.05 mg/ml gentamicin and stored on ice. Then the sieves were backwashed, and myometrial and glandular debris were further digested to single cells for 45 min as described above. All cell suspensions were filtered as described above, and combined. To remove erythrocytes, the cells were resuspended in 500 μl of HLB solution (Immuno Biological Laboratories) and incubated for 3 min. After washing twice with PBS, viable cell numbers were counted with trypan blue (Sigma–Aldrich). Cells were seeded on gelatin (0.1%, Sigma–Aldrich)-coated dishes at various densities of $0.1–3 \times 10^5$ cell/60-mm dish. After 14 days, non-overlapping clones were distinguished. Primary cell clones were expanded in DMEM/F-12 containing 5% FBS (SAFC Biosciences) and 0.05–0.1 mg/ml gentamicin, on gelatin-coated dishes.

2.5. Serial cloning of colony-forming cell clones

Self renewal was assessed by serial cloning of individual clones as described by Gargett et al. [18]. Cells were seeded on gelatin-coated 100-mm dishes at 10 cells/cm^2 (600 cells/100-mm dish). Culture medium was changed every 4 days and secondary clones formed distinct colonies by 14 days after plating. Secondary clones were similarly recloned to generate tertiary clones, and were also expanded in the same manner as the primary culture.

2.6. In vitro genistein exposure to colony-forming cells

From 70 isolated cell clones, we selected 20 clones from colonies that were composed of fibroblastic-shaped, homogenous cells with an average doubling time of less than 100 h. The selected clonal cells, whose passage number was less than 10, were subjected to *in vitro* GEN exposure. Cells were seeded on gelatin-coated 60-mm dishes, treated with or without 10 μM of GEN (dissolved in dimethylsulfoxide (DMSO)) in DMEM/F-12 containing 5% FBS and 0.05 mg/ml gentamicin for 7 days. The final DMSO concentration was 0.02%. The culture medium was changed every 2 days.

2.7. Genomic DNA preparation and bisulfite sequencing

Genomic DNA was isolated using a QIAamp DNA Mini Kit (QIAGEN) and 180 ng–1 μg was subjected to sodium bisulfite modification with a EpiTect Bisulfite Kit (QIAGEN) according to manufacturer's protocols. Bisulfite sequencing primers are shown in Supplementary Table 1. PCR products were cloned into the pT7 blue T vector (Novagen) and transformed into *Escherichia coli*. Plasmid DNA from positive colonies was purified and sequenced at the Tokyo Medical and Dental University Genome Laboratory (Tokyo, Japan). Sequence and statistical analyses were performed with the QUantification tool for Methylation Analysis; http://quma.cdb.riken.jp/top/quma_main_j.html [19]. The statistical significance of the difference between two bisulfite sequence groups at each CpG site was evaluated with Fisher's exact test.

2.8. Screening of DNA methylation status by high-resolution melting assay

All assays were performed on the LightCycler 480 using the LightCycler 480 High Resolution Melting Master kit, according to the manufacturer's instructions. Primers, designed using LightCycler Probe Design Software 2.0 (All, Roche Applied Science) are shown in Supplementary Table 1. All data were analyzed using LightCycler Gene Scanning Software.

2.9. Statistical analysis

Data are shown as means ± SD. Unpaired *t*-tests were used to compare the significance between two groups. Statistical analysis

was performed using Dr. SPSS 2 for Windows. Results were considered statistically significant at a P value of <0.05.

3. Results

3.1. Effects of genistein in uteri of ovariectomized (OVX) mice

OVX mice were fed with either vehicle (control) or low (60 mg/kg) or high (200 mg/kg) doses of GEN for 7 days and blotted uterus weights were determined (Fig. 1A). Compared to the control, low-dose GEN treatment did not significantly increase the uterus weight; high-dose treatment induced a slight but significant uterus enlargement (1.4-fold of control; $P < 0.005$). We then determined the mRNA expression levels of SF-1 (Fig. 1B) and steroidogenic genes (Fig. 1C–F) by the Percellome method. The mRNA levels of these genes were very low in the endometria from control and low-dose GEN-treatment groups, but were significantly increased (still less than one copy per cell on average) in the high-dose treatment group ($P < 0.05$), indicating that high-doses of GEN induced expression of these genes. Next, we determined the methylation status of SF-1 in

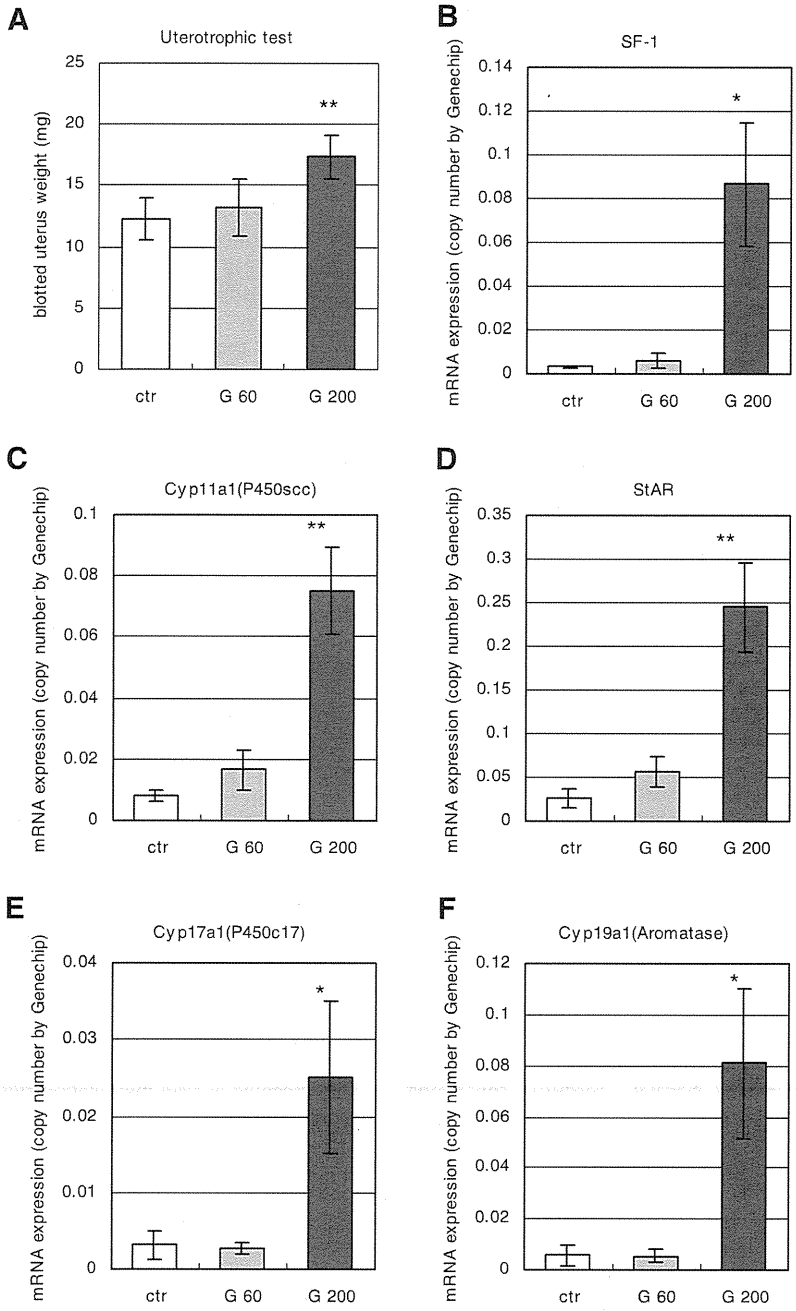

Fig. 1. Genistein induced endometrial regeneration and SF-1 mRNA expression in uterine tissue of OVX mice. (A) Blotted uterine weights were recorded. Control and GEN-treated groups comprised five and four mice, respectively. ctr; control, G 60; GEN 60 mg/kg/d, G200; GEN 200 mg/kg/d. (B–F) mRNA expressions of steroidogenic genes were determined using GeneChip analysis and were calculated by the Percellome method. *Y* axis indicates mRNA expression as copy number per cell. (B) SF-1 was determined by 1418315_at, (C) Cyp11a1 by 1439947_at, (D) StAR by 1418729_at, (E) Cyp17a1 by 1417017_at, and (F) Cyp19a1 by 1449920_at. *Statistically significant at $P < 0.05$. **Statistically significant at $P < 0.005$.